European Radiology (2019) 29:4572–4582
https://doi.org/10.1007/s00330-018-5899-8

CARDIAC

Noise reduction and motion elimination in low-dose 4D myocardial computed tomography perfusion (CTP): preliminary clinical evaluation of the ASTRA4D algorithm

Steffen Lukas[1] · Sarah Feger[1] · Matthias Rief[1] · Elke Zimmermann[1] · Marc Dewey[1]

Received: 27 June 2018 / Revised: 15 October 2018 / Accepted: 20 November 2018 / Published online: 4 February 2019

Abstract

Objectives To propose and evaluate a four-dimensional (4D) algorithm for joint motion elimination and spatiotemporal noise reduction in low-dose dynamic myocardial computed tomography perfusion (CTP).

Methods Thirty patients with suspected or confirmed coronary artery disease were prospectively included and underwent dynamic contrast-enhanced 320-row CTP. A novel deformable image registration method based on the principal component analysis (PCA) of the ante hoc temporally smoothed voxel-wise time-attenuation curves (ASTRA4D) is presented. Quantitative (standard deviation, signal-to-noise ratio (SNR), temporal variation, volumetric deformation) and qualitative (motion, contrast, contour sharpness [1, poor; 5, excellent]) measures of CTP quality were assessed for the original and motion-compensated sequences (without and with temporal filtering, PCA/ASTRA4D). Following myocardial perfusion deficit detection by two readers, diagnostic accuracy was evaluated using magnetic resonance myocardial perfusion imaging (MR-MPI) as the reference standard in 15 patients.

Results Registration using ASTRA4D was successful in all 30 patients and resulted in comparison with the benchmark PCA in significantly ($p < 0.001$) reduced noise over time (− 83%, 178.5 vs 29.9) and spatially (− 34%, 21.4 vs 14.1) as well as improved SNR (+ 47%, 3.6 vs 5.3) and subjective image quality (motion, contrast, contour sharpness [+ 1.0, + 1.0, + 0.5]). ASTRA4D had significantly improved per-segment sensitivity of 91% (58/64) and similar specificity of 96% (429/446) compared with PCA (52%, 33/64; 98%, 435/446; $p = 0.011$) in the visual detection of perfusion deficits.

Conclusions The ASTRA4D registration algorithm improved the spatiotemporal noise profile and CTP sequence image quality, resulting in significantly improved sensitivity of 4D CTP in the detection of myocardial ischemia.

Key Points

- *ASTRA4D combines local temporal regression and deformable image registration.*
- *Quantitative and qualitative measures of CTP quality are improved compared to PCA.*
- *Improved spatiotemporal differentiation of ischemic regions leads to an excellent perfusion deficit concordance of ASTRA4D with MRI.*

Keywords Coronary artery disease · Computed tomography myocardial perfusion imaging · Temporal averaging · Motion artifacts · Deformable registration

Abbreviations

CAD	Coronary artery disease
CT	Computed tomography
CTP	Computed tomography perfusion
HU	Hounsfield unit
IQR	Interquartile range
MPI	Myocardial perfusion imaging
MR	Magnetic resonance
PCA	Principal component analysis

Electronic supplementary material The online version of this article (https://doi.org/10.1007/s00330-018-5899-8) contains supplementary material, which is available to authorized users.

✉ Marc Dewey
dewey@charite.de

[1] Department of Radiology, Charité Medical School, Charitéplatz 1, 10117 Berlin, Germany

ROI Region of interest
TAC Time-attenuation curve
WL Window level

Introduction

Cardiovascular disease is the leading global cause of mortality [1], accounting for 31% of all deaths worldwide according to the World Health Organization. While computed tomography angiography (CTA) is the most accurate noninvasive modality for detecting coronary artery stenosis in the clinical setting, it lacks the ability to assess its hemodynamic significance [2]. Evaluation of cardiac perfusion by contrast-enhanced computed tomography perfusion (CTP), on the other hand, has been shown to improve diagnostic accuracy for the detection of functionally relevant coronary artery disease (CAD) [2–5], hitherto mostly assessed by stress myocardial perfusion imaging (MPI), using magnetic resonance (MR), positron emission tomography, or single photon emission computed tomography as the noninvasive perfusion imaging reference standard [6–9]. Recent advances in 4D CTP acquisition protocols (e.g., low kV), technology, availability, and cost-effectiveness may render CT the adequate basis for joint anatomical and functional assessment at high diagnostic accuracy in a single modality [2, 10, 11]. But, radiation exposure from repeat scans (e.g., 9 mSv in our pilot study [12]), intrinsic artifacts from concurrent patient motion and cardiac deformation, beam hardening from highly attenuating tracer, lack of standardization of perfusion imaging biomarkers, and difficult postprocessing have so far hindered CTP from becoming a routine diagnostic test.

This study investigates the ability of CT-MPI to identify potential myocardial ischemia on the basis of enhanced hypoattenuation during stress compared to rest imaging. Perfusion deficit detection may be complicated by motion artifacts, especially in stress imaging with higher heart rates, noise from low-voltage scatter radiation, and wide detector array. Plain filtering without motion correction [12–14] may result in degraded image quality from motion-induced blurring. While several principal component-based dimension reduction techniques have been successfully applied in reducing motion while separating it from tracer-induced intensity changes [15–19], they do not ensure temporal smoothness without explicit regularization. Post hoc spatiotemporal filtering following motion compensation [20, 21] improves the noise profile but is not formally embedded in a registration framework.

The aim of the present study was, first, to combine temporal noise reduction and motion elimination of the entire 4D low-dose cardiac CT perfusion sequence in a unified framework on the basis of exploratory principal component-based alignment [17] using an ex ante approach to temporal smoothing and, second, to investigate the added diagnostic value in an initial clinical analysis in patients with confirmed or suspected CAD.

Materials and methods

Patients

After obtaining ethical approval and written informed consent, 30 patients (aged 63 ± 11) with confirmed or suspected CAD and an indication for cardiac CT perfusion were included in our earlier prospective 4D CTP pilot study [12], where details on inclusion and exclusion criteria and patient preparation can be found. In the study presented here, we rely on the same patient cohort whose characteristics are recapitulated in Table 1 for convenience.

CT examination protocol

All patients underwent both coronary CTA and stress dynamic myocardial CTP after vasodilator administration (320-row,

Table 1 Four-dimensional CTP patient characteristics and examination protocol

Patient characteristics CT-MPI	
No. of patients	30
Age, years	63 ± 11
Male sex, *n* (%)	26 (87)
Height, m	1.73 ± 0.08
Weight, kg	82 ± 13
Body mass index	27 ± 3
CT examination protocol	
Oral β-blocker, *n* (%)	19 (63)
i.v. β-blocker, *n* (%)	7 (23)
Heart rate during CTA, bpm	49 ± 5
Heart rate during CTP, bpm	73 ± 12
Tube current CTA, mA	353 ± 60
Tube voltage CTA, kV	120 ± 5
Tube current CTP, mA	142 ± 11
Tube voltage CTP, kV	103 ± 8
Contrast amount CTA, ml	58 ± 0
Contrast amount CTP, ml	42 ± 0
Injection rate, ml/s	7.0 ± 0
Gantry rotation time, ms	350
RR cycle scan interval, %	70–80
Number of heartbeats CTP	20 ± 3
Effective dose CTA, mSv	3.1 ± 2.0
Effective dose CTP, mSv	9.3 ± 1.9

Aquilion One, Canon Medical Systems, 16 cm scan coverage, spatial resolution 0.35 × 0.35 × 0.25 mm^3, rotation time 0.275 s). CTA was performed at a tube voltage of 120 ± 5 kV and a tube current of 353 ± 60 mA. CTP followed CTA and was initiated after 3 min of continuous intravenous infusion of a body weight-adjusted dose of adenosine into the left cubital vein at a rate of 140 μg/kg/min. The 4D CTP datasets were acquired at a gantry rotation time of 350 ms with a tube voltage of 103 ± 8 kV and a tube current of 142 ± 11 mA, resulting in an effective dose of 3.1 ± 2.0 mSv for CTA and 9.3 ± 1.9 mSv for CTP.

For both scans (CTA and CTP), a total of 58 ml nonionic iodinated contrast agent (iobitridol, 350 mg/ml, Xenetix 350, Guerbet) for CTA and 42 ml for CTP was injected through the right antecubital vein and was followed by an 80 ml saline flush, both administered at a flow rate of 7 ml/s. No special contrast administration system was employed, and large intravenous access was sufficient. Dynamic CTP acquisition was started using CTA bolus tracking (2 s before bolus arrival in the left ventricle). Dynamic scanning was performed at 70–80% of the RR interval with one acquisition every heartbeat over a period of up to 20 heartbeats, followed by three single late phases (10 s, 20 s, and 35 s) after the last acquisition. Heart rate was 49 ± 5 bpm during the CTA scan and 73 ± 12 bpm during the CTP scan.

MR examination protocol

Cardiac first-pass magnetic resonance imaging (MRI) was performed in 15 of the 30 pilot study patients as clinically indicated, after excluding patients with contraindications to MRI [12]. Three cardiac short-axis views (basal, midventricular, apical) and one long-axis view were obtained for a total of 60 segments on a 1.5-T MR scanner (Magnetom Avanto, Siemens Healthineers, integrated motion correction) using a steady-state coherent sequence with balanced gradients (SR TrueFISP, 2 mm in-plane resolution, 8 mm slice thickness). First, two quantitative rest perfusion scans were performed after intravenous infusion of contrast agent (3 ml at 4 ml/s and 6.3 ml/s, Dotarem, Guerbet). Second, after adenosine administration (140 μg/kg/min over 4:30 min, Adenosin Life Medical, Carinopharm, 3 mg/ml) as a pharmacological vasodilator, stress MRI was conducted in two quantitative scans (same tracer amount and flow rates), finally followed by qualitative stress and rest scans (0.2 ml/kg body weight minus 6 ml at 4 ml/s) resulting in a total dose of 0.2 mmol gadoterate meglumine/kg body weight.

CT image postprocessing

Each 3D volume was reconstructed independently with the strong level of the adaptive iterative dose reduction 3D algorithm (AIDR 3D, Canon Medical Systems [22]) using an imaging matrix of 512 × 512 pixels at 75% of each RR interval. The acquisition field of view (FOV) was 187 ± 10 mm in *x*/*y*-direction and 120 ± 8 mm in *z*-direction. For the purpose of this study, volumes were downsampled 30-fold from 0.35 × 0.35 × 0.25 to 1 mm^3 isotropic resolution.

The proposed ASTRA4D algorithm

The aim of the algorithm proposed here is twofold: first, to spatially align the entire sequence and, second, to reduce noise. Aligned anatomical structures result in intensity curves with smooth variation over time, which are disturbed by noise incurred from low-dose acquisition as well as patient motion and cardiac deformation. Contrary to postregistration temporal filtering (as in [20, 21]), we chose to embed smoothing into the registration process itself in an attempt to robustly recover the underlying anatomical structures. Therefore, our algorithm involves the creation of an interim-smoothed sequence based on the current deformed cardiac volumes. Local polynomial regression was used as a linear smoothing method to noise-reduce interim time-attenuation curves (TACs). Residuals are weighted locally by a Gaussian kernel penalizing deviation from current time points (Fig. 1A). Kernel bandwidth choice entails a trade-off between temporal smoothness and fit to acquired data (Fig. 1B). In the limiting case of zero kernel bandwidth, we merely interpolate. Both improved voxel-wise temporal smoothness and morphological alignment result in a more condensed representation of the eigenvalues of the intervolume correlation matrix (Fig. 1C, D) obtained from a principal component analysis (PCA). These two goals of perfusion sequence registration can thus be tackled simultaneously using the same target metric: the inversely weighted sum of the spectrum of the correlation matrix (see Electronic Supplementary Material (ESM) for a detailed technical explanation). Only the latter, morphological alignment, has been targeted within the benchmark method [17]. Going beyond, the ASTRA4D algorithm combines temporal regression and spatial alignment: the registration process seeks the deformable transformation such that deformed and smoothed volumes can be described by few dominant principal components, thus removing temporal noise and motion artifacts at the same time. The result of the registration is the smooth interim sequence. The bandwidth for ASTRA4D of 2.0 has been justified empirically, see ESM for details; the benchmark PCA corresponds to the limiting case of 0.0.

CT myocardial perfusion sequence analysis

To assess quantitative, qualitative, and diagnostic registration quality, three datasets were generated for each patient: the original series without motion correction (ORG), the motion

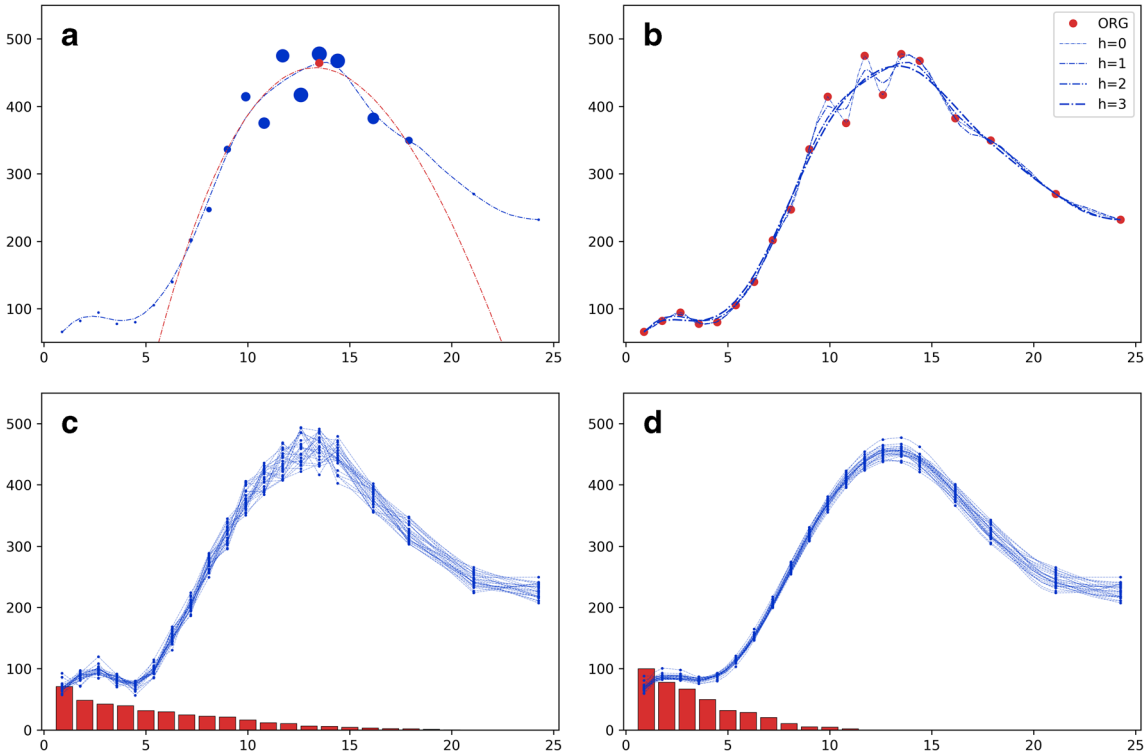

Fig. 1 ASTRA4D methodology. Illustration of temporal regression. **a** Local polynomial regression (LPR) at the selected time point (red circle) with local cubic fit (red) to data points (blue) with Gaussian weights (size proportional to weight). **b** LPR fit of data points (red) for different bandwidths. **c** Twenty-six random perturbations of the original aortic TAC and their corresponding correlation spectrum (red). **d** Temporally smoothed TACs and their spectrum. As a result of smoothing, joint evolution of TACs can be explained with a few leading eigenvectors

compensated series using the benchmark method (PCA [17]), and the proposed simultaneously motion- and noise-reduced sequence (ASTRA4D).

Quantitative analysis

Four distinct cuboid regions in the myocardium ($3 \times 3 \times 3$ mm^3) of the left ventricular wall were marked in the volume of the original sequence where the lumen of the left ventricular chamber just exceeded that of the right ventricular chamber and mapped into the respective registration-implicit reference frame. We evaluated the following quality measures using 5 levels of temporal smoothing (0, 1, 2, 3, 4), each aggregated per region of interest (ROI) over time: image noise as standard deviation (SD; Hounsfield unit, HU), signal-to-noise ratio (SNR) as the ratio of mean signal over noise, temporal variation (TV) as the average curvature along each TAC (mean squared second temporal derivative), volumetric deformation (VD; percent) as the average volumetric change (Jacobian determinant of the transformation model underlying the deformable registration), and mean deviation (MD; HU) as the mean TAC difference with respect to the benchmark (PCA).

Qualitative analysis

Visual image quality of the animated CTP sequences (ORG, PCA, ASTRA) for all 30 patients was subjectively graded (motion, contrast, contour sharpness) by two independent readers (same as perfusion analysis, blinded to the registration method and in random order) in axial views on a 5-point scale (1 = poor, 5 = excellent). Slice thickness, window level, and frames per second (FPS) could be freely adjusted (preset settings 1 mm, WL 400/100, FPS 8). The grades were averaged between readers for each measure and patient.

Perfusion analysis

Semi-quantitative visual assessment of myocardial perfusion (normal vs hypoperfusion) was performed for each sequence (qualitative stress MR-MPI and 4D CTP) by two experienced radiologists at our institution (blinded to the clinical information and registration method and in random order), in cardiac short-axis and long-axis views for the subcohort (15/30) which underwent both examinations. The readers were allowed to adjust freely cardiac orientation and preset window settings (WL 200/100 [23], slice thickness 4 mm). The time lag between CT and MR readings was 6 months and

12 months, respectively, thus minimizing memory effects. Myocardial segments and major coronary branches (LAD; RAD; LCX) were identified using the 17-segment model (American Heart Association guidelines [24]). The ground truth for the occurrence of myocardial perfusion deficits in the MR-MPI sequences was agreed upon by consensus. Diagnostic performance was evaluated as sensitivity and specificity (reported including numerator and denominator) individually for each reader as well as combined on a per-patient, per-vessel, and per-segment basis considering the MR-MPI consensus reading as the reference standard.

Statistical analysis

All variables are reported as median and interquartile range (IQR) if not indicated otherwise. Normal distribution was assessed using the Shapiro-Wilk test. Intermethod performance was statistically compared using the paired Wilcoxon signed-rank test. Interobserver agreement was determined using the kappa statistic. Heterogeneity in the detection of myocardial perfusion deficits was assessed using Cochran's Q test. All statistical analyses were performed using Python 2.7. Differences were considered to be statistically significant at p values less than 0.05.

Results

The study population consisted of 30 patients with confirmed or suspected CAD. All 4D CTP sequences were successfully registered using the designated bandwidths. Figure 2 exemplifies the visual image quality of the three sequences for a cardiac long-axis view in comparison to MR (8 mm; in addition, ESM Video 1). Figure 3 illustrates spatiotemporal motion and noise for the three sequences by temporally selected axial slices and their corresponding color-coded difference images.

Quantitative analysis

Quantitative image quality measures are detailed in Table 2. The use of ASTRA4D significantly reduced temporal variation by 83% (178.5/119.2 vs 29.9/12.0) and spatial standard deviation by 34% (21.4/7.6 vs 14.1/6.8) and increased signal-to-noise ratio by 47% (3.6/2.5 vs 5.3/3.2) in the myocardium compared to the benchmark PCA (all $p < 0.001$; median/interquartile range). In contrast, PCA alone reduced temporal variation by 2% (178.5/119.2 vs 182.2/139.5) and standard deviation by 9% (21.4/7.6 vs 23.5/8.8), while it increased signal-to-noise ratio by 9% (3.6/2.5 vs 3.3/2.6) compared to the original unregistered CTP sequence (all $p < 0.001$). ASTRA4D introduced neither a systematic intensity bias along the TACs compared to the PCA method (mean deviation 0.0/0.9 HU, $p < 0.001$) nor strong spatial distortions in myocardial target regions (volumetric deformation 0.2/3.3, $p = 0.51$). ESM Figure 1 shows the three quantitative measures (TV, SD, SNR) for different bandwidths in relation to those obtained from the original sequence.

Qualitative analysis

Qualitative image quality measures are detailed in ESM Table 1. Interreader agreement on image quality scores for all CTP sequences (ORG, PCA, ASTRA) between the two readers was substantial (mean $\kappa = 0.75$) for all three measures (motion, contrast, contour sharpness), ratings differed by one point maximally. ASTRA4D significantly improved subjective perfusion sequence image quality compared to both the original sequence (motion, contrast, and contour sharpness at 1.0/1.4, 1.0/0.5, and 0.5/1.0, respectively; $p < 0.001$) and the benchmark method PCA (motion, contrast, and contour sharpness at 1.0/1.8, 1.0/1.5, and 0.5/1.0, respectively; $p < 0.001$). Likert plots for each qualitative measure and dataset are depicted in Fig. 4. On a voxel-wise level, zig-zag curves already present in the original series may show slightly less variation after motion compensation by PCA; however, overall shape is not rectified (Fig. 5, right panel), which can only be achieved by the additive use of temporal regularization as in ASTRA4D. In some cases, this behavior of PCA can even lead to a fluctuating anatomy in the registered series (Video 2, ESM), which may be considered an intrinsic

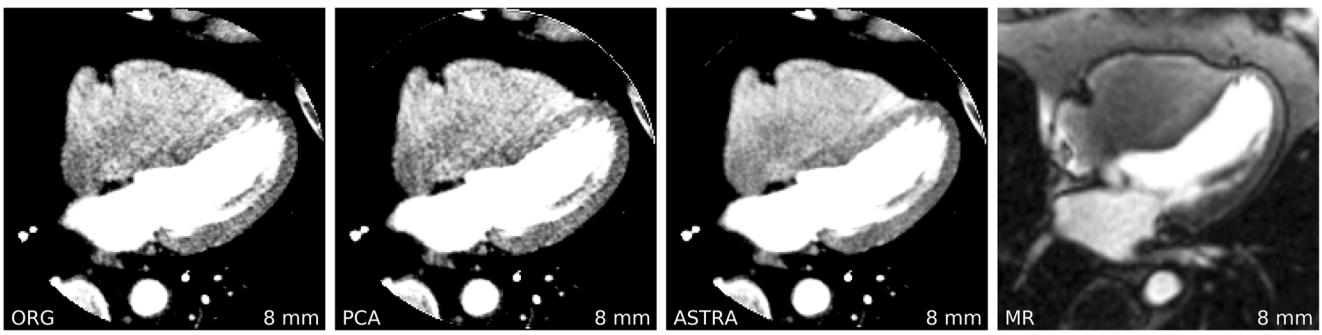

Fig. 2 Image quality of ASTRA in comparison to the reference methods. Long-axis views of CT (8 mm; WL 200/100) and MR (WL 100/50) exemplifying improved 4D CTP image quality using ASTRA

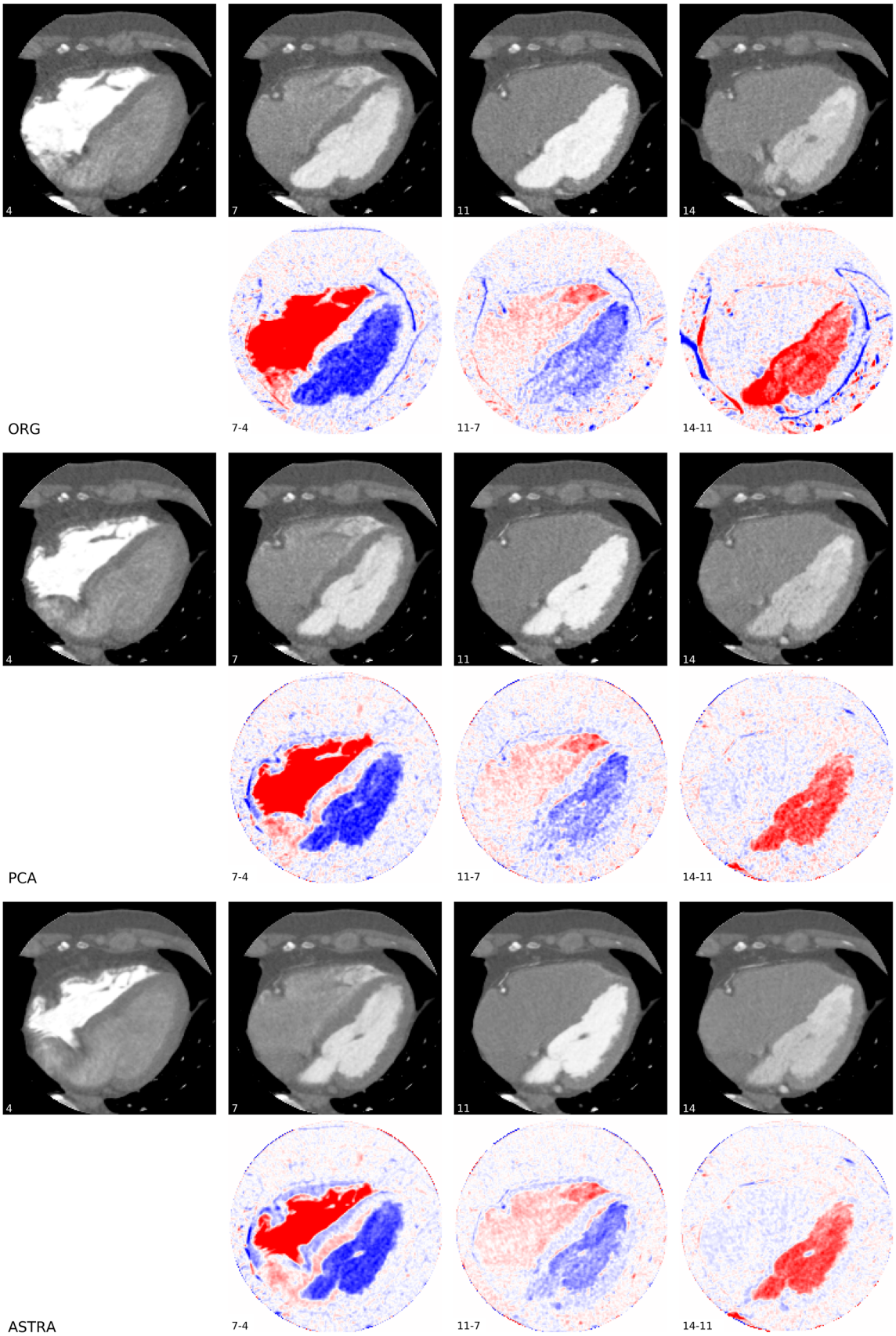
4
7
11
14
7-4
11-7
14-11
ORG
PCA
ASTRA

◀ **Fig. 3** Cardiac 4D CTP sequence and difference images. Representative axial slices and corresponding color-coded difference images underneath (CTP WL 1300/200, difference sequence WL 900/0). While PCA already reduces motion as seen in the difference image, ASTRA4D, in addition, reduces noise. The misalignment between different phases can be detected visually by the presence of edges in the difference images (ORG) for tissues of substantially different attenuation, e.g., the heart and lung or myocardium and ventricle

artifact of PCA. Sequential difference images in Fig. 3 beautifully illustrate how the combination of motion reduction and spatiotemporal denoising confines contrast differences to regions of tracer flux (bottom row), thus improving the differentiation of hypoperfused from healthy myocardial tissue (see Fig. 6 for a representative patient). Smooth voxel-wise TACs (Fig. 5, bottom row) lead to higher perfusion deficit persistence over time in ASTRA4D (Video 1, ESM).

Perfusion analysis

Interreader agreement on the presence of MR hypoperfusion among the two readers was excellent ($\kappa = 0.93$ on a per-segment basis), with four deviating neighboring segments in total. Concordance in CT deficit reading was excellent ($\kappa =$ 0.97, 0.85, and 0.98 on a per-segment basis for ORG, PCA, and ASTRA, respectively). Higher temporal persistence and more precise delineation of myocardial perfusion defects from using ASTRA, as illustrated in Fig. 6, lead to a diagnostic performance of perfusion CT that is similar to that of perfusion MR in the detection of myocardial perfusion deficits (Table 3). Using ASTRA4D, sensitivity and specificity on a per-vessel basis were 100% (36/36) and 93% (50/54), while 91% (58/64) and 96% (429/446) on a per-segment basis, respectively. Reading of the PCA-motion–corrected series was significantly less sensitive with a sensitivity of 56% (20/36), while the specificity was similar with 91% (49/54) on a per-vessel basis ($p = 0.010$) and 52% (33/64) and 98% (435/446) on a per-segment basis ($p = 0.011$). For a complete overview of segment-wise myocardial deficits for all sequences, please see ESM Table 2.

Discussion

The ASTRA4D method presented here aimed to investigate the potential of local temporal regression for improved myocardial deficit detection in cardiac low-dose CTP in addition to motion compensation alone without temporal regularization. Our initial clinical evaluation ($n = 30$) shows that improved temporal persistence and differentiation of the hypoperfused myocardium resulting from the use of ASTRA4D lead to a diagnostic performance similar to that of perfusion MR imaging in the visual detection of myocardial perfusion deficits (Table 3). The additional use of temporal filtering in ASTRA resulted in a significantly more sensitive visual detection of perfusion deficits than the benchmark method PCA (with a sensitivity of 91% compared to 52% on a per-segment basis) with the noninvasive reference standard MR-MPI. Reading in the uncorrected sequence was only slightly worse sensitive than the PCA benchmark, which exceeds, however, the deficit detection using uniform interphase averaging without motion correction [12] with a mere sensitivity of 31%. The absence of spatiotemporal regularization in PCA may lead to artifacts, and cardiac deformation and patient motion can blur averaged volumes when no prior motion correction is used. As a result, diagnostic performance is degraded in both cases. A related study comparing dynamic perfusion CT and MR [25] for the detection of myocardial perfusion deficits reported a diagnostic accuracy of 100/75% per vessel and 78/76% per segment (sensitivity/specificity, $n = 31$, dual-source CT 2 × 100 kV, 73 mm detector array, spatial resolution 0.3 mm, rotation time 0.28 s, 11 ± 2 mSv; 3 T MR, in-plane 2.8 mm, slice

Table 2 Quantitative evaluation

Measure	ORG	PCA	ASTRA4D			
Bandwidth		0	1	2	3	4
Temporal variation (TV)*	182.2 (139.5)	178.5 (119.2)	90.8 (33.6)	29.9 (12.0)	13.8 (8.0)	7.0 (3.5)
Standard deviation (SD)*	23.5 (8.8)	21.4 (7.6)	18.0 (7.0)	14.1 (6.8)	12.7 (6.8)	12.0 (7.1)
Signal-to-noise ratio (SNR)*	3.3 (2.6)	3.6 (2.5)	4.2 (2.7)	5.3 (3.2)	5.8 (3.7)	6.2 (4.0)
Mean deviation (MD)*	–	0.0 (0.0)	− 0.0 (0.3)	− 0.0 (0.9)	0.0 (1.7)	− 0.0 (2.2)
Volumetric deformation (VD)**	–	0.2 (3.0)	0.2 (3.2)	0.2 (3.3)	0.2 (3.4)	0.2 (3.4)

Quantitative measures of different registrations and the original sequence (ORG) in the myocardium for different kernel bandwidths (0–4): temporal variation (TV), standard deviation (SD), signal-to-noise ratio (SNR), mean deviation (MD), and volumetric deformation (VD). Median and interquartile range

*$p < 0.001$; **$p = 0.26$, 0.51, 0.38, and 0.23 for bandwidths 1, 2, 3, and 4, in relation to the benchmark (PCA; column 0)

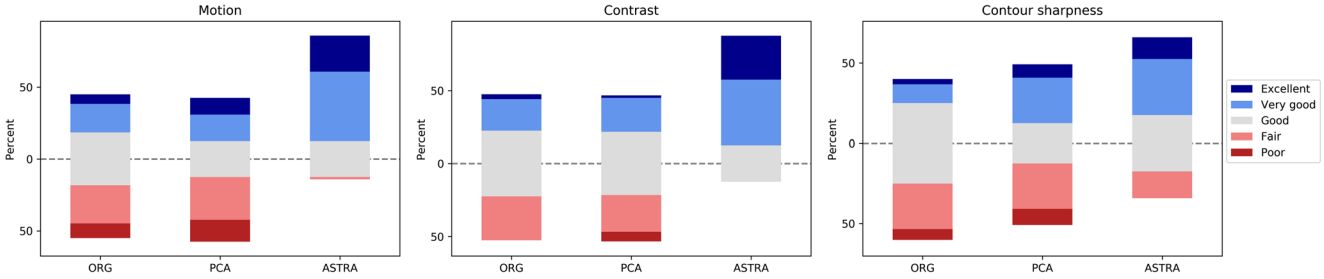

Fig. 4 Qualitative evaluation. Comparison of subjective image quality in terms of motion, contrast, and contour sharpness on a 5-point Likert scale (1 = poor, 5 = excellent). ASTRA4D significantly reduced motion (left; + 1.0 vs ORG and PCA) and improved contrast (middle; + 1.0 vs ORG and PCA) and contour sharpness (right; + 0.5 vs ORG and PCA)

thickness 10 mm, linearly ordered saturation recovery fast spoiled gradient echo protocol).

ASTRA4D improved both subjective and objective measures of perfusion sequence image quality in comparison to the benchmark method PCA (motion + 1.0, contrast + 1.0, contour sharpness + 0.5; temporal variation − 83%, standard deviation − 34%, SNR + 47%; $p < 0.001$) by simultaneously imposing temporal smoothness and anatomic alignment. Similar findings for the myocardium are reported by [21] (standard deviation − 65%, 80 kV, temporal 3-point weighted moving average filter and edge-preserving spatial filtering, 7.1 ± 1.1 mSv, $n = 2$) and [20] (SNR + 62%, Karhunen-Loève transform filtering), both applying postregistration spatiotemporal noise reduction. Muenzel et al [21] also reported improved differentiation of normal and ischemic myocardium; however, post hoc spatiotemporal filtering itself may also introduce artifacts [20]. Our ante hoc temporal regression may be seen as a justification of post hoc temporal filtering approach by embedding it into a unified motion compensation framework, comprising both motion elimination and noise reduction. Minor cardiac arrhythmia will be tolerated and is accounted for in the algorithm by registering to a mean reference frame and thus eliminating possible cardiac RR mistiming.

Myocardial perfusion CT imaging has a relatively poor contrast resolution, and the HU difference between normal and hypoperfused myocardium remains small, in the range of 17–50 HU [26] after bolus injection. A relatively high infusion rate of 7 ml/s was used to ensure visual myocardial deficit readability in the uncorrected CTP sequence from increased peak myocardial enhancement.

In our retrospective study, spatial filtering as a method of dose reduction was already embedded in the independent reconstruction of the cardiac volumes prior to registration

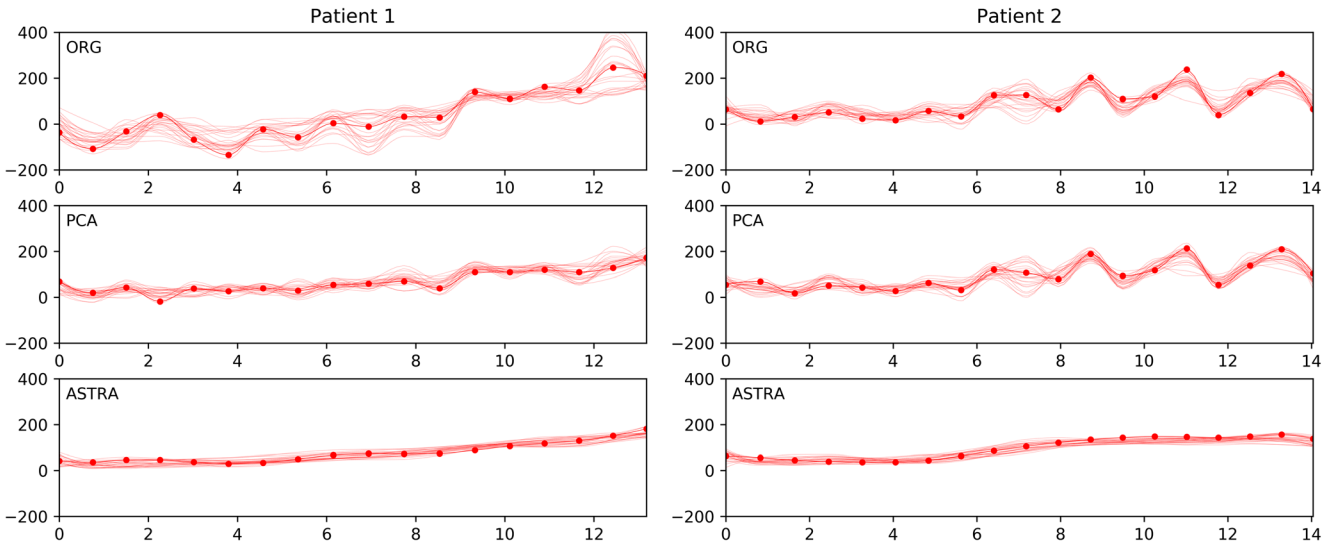

Fig. 5 Four-dimensional CTP TAC-wise motion elimination using PCA and ASTRA4D. Four-dimensional CTP voxel-wise myocardial TACs in a region of 3 × 3 × 3 mm^3. Central TAC (solid red line) and its 26 adjacent TACs (dotted). The left panel shows that motion can be successfully removed using PCA; in addition, ASTRA reduces noise. However, zigzag curves of the original sequence, on the right panel, cannot be resolved by PCA alone. Only the use of temporal regularization in conjunction with motion correction, as in ASTRA, allows the generation of persistent and well-delineated ischemic regions from the original sequence

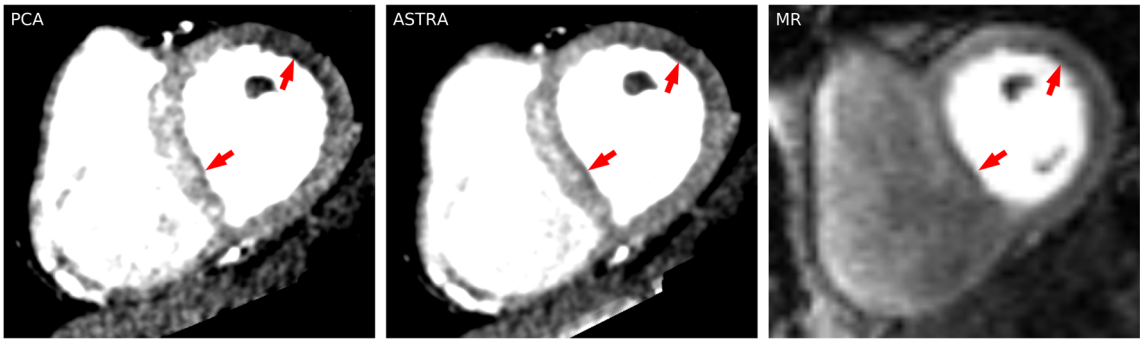

Fig. 6 Delineation of ischemia by 4D CTP using ASTRA4D compared to MR-MPI. Four-dimensional CTP and MR basal short-axis views (PCA, ASTRA, WL 146/108, slice thickness 8 mm). Myocardial hypoperfusion in basal segments (inferoseptal, inferolateral, and anterolateral [three, five, and six, respectively]) is correctly identified (arrows) and illustrates precise differentiation of hypoperfused areas in this representative patient. MR (WL 100/50) was acquired in a more diastolic phase and CT in a more systolic phase

(AIDR 3D, Canon Medical Systems, iterative adaptive weighted anisotropic diffusion filtering [27]). ASTRA4D, on the other hand, achieves noise reduction by applying a regression in temporal domain, which may equally get translated into prospective radiation dose savings. Whole-heart CTP acquisitions may become technically feasible at < 3 mSv by combining low-current, low-voltage temporally undersampled acquisition [28, 29] with postprocessing methods, such as ASTRA4D, embracing the true spatiotemporal nature of time-resolved imaging.

There are limitations to our study. Only 30 patients were analyzed in a preliminary retrospective clinical evaluation of a pilot study, and further studies are required to validate the incremental value. Visual analysis of perfusion deficits is certainly limited by its subjective nature, despite excellent interreader agreement. Quantitative analysis of perfusion would probably be a more accurate analysis; it has not yet evolved, however, to be routinely used in clinical practice. We used a uniformly downsampled resolution of 1 mm, resulting in reasonably well-behaved myocardial TACs amenable to temporal regression, a moderate restriction taking into account the extent of ischemic regions. The extension to include a spatiotemporal kernel with a sufficiently narrow spatial bandwidth would be straightforward, albeit computationally more expensive. No formal assessment of registration accuracy with respect to a given ground truth, necessarily both deformation and intensity change, was done. Our method, however, does not introduce a bias with respect to the PCA benchmark ([17, Table 7], DICE 52 ± 13, $n = 9$). Technically, both components of our method, PCA and temporal regression, are linear in nature. The application of PCA implicitly assumes a linear model of contrast agent propagation. Further gains in registration performance are to be expected from the transition to nonlinear and higher dimensional techniques.

In conclusion, ASTRA4D adds value in postprocessing by providing an aligned dataset with spatiotemporally improved image quality for any dynamic contrast-enhanced examination and it is shown here to improve quality metrics and sensitivity of cardiac 4D CTP. Better differentiation and higher temporal persistence of ischemic myocardial tissue enable accurate detection of myocardial perfusion deficits. The method may foster the role of CT as an imaging tool for the

Table 3 Diagnostic comparison of 4D CT with MR-MPI as the reference standard

Diagnostic accuracy	CT reader 1			CT reader 2			Combined		
	ORG	PCA	ASTRA	ORG	PCA	ASTRA	ORG	PCA	ASTRA
Per patient ($n = 15$)									
Sensitivity, %	64 (7/11)	64 (7/11)	100 (11/11)	73 (8/11)	73 (8/11)	100 (11/11)	68 (15/22)	68 (15/22)	100 (22/22)
Specificity, %	100 (4/4)	75 (3/4)	100 (4/4)	100 (4/4)	75 (3/4)	100 (4/4)	100 (8/8)	75 (6/8)	100 (8/8)
TP/FP/FN/TN	7/0/4/4	7/1/4/3	11/0/0/4	8/0/3/4	8/1/3/3	11/0/0/4	15/0/7/8	15/2/7/6	22/0/0/8
Per vessel ($n = 45$)									
Sensitivity, %	56 (10/18)	50 (9/18)	100 (18/18)	61 (11/18)	61 (11/18)	100 (18/18)	58 (21/36)	56 (20/36)	100 (36/36)
Specificity, %	100 (27/27)	89 (24/27)	93 (25/27)	100 (27/27)	93 (25/27)	93 (25/27)	100 (54/54)	91 (49/54)	93 (50/54)
TP/FP/FN/TN	10/0/8/27	9/3/9/24	18/2/0/25	11/0/7/27	11/2/7/25	18/2/0/25	21/0/15/54	20/5/16/49	36/4/0/50
Per segment ($n = 255$)									
Sensitivity, %	44 (14/32)	47 (15/32)	91 (29/32)	47 (15/32)	56 (18/32)	91 (29/32)	45 (29/64)	52 (33/64)	91 (58/64)
Specificity, %	98 (219/223)	97 (217/223)	96 (215/223)	98 (219/223)	98 (218/223)	96 (214/223)	98 (438/446)	98 (435/446)	96 (429/446)
TP/FP/FN/TN	14/4/18/219	15/6/17/217	29/8/3/215	15/4/17/219	18/5/14/218	29/9/3/214	29/8/35/438	33/11/31/435	58/17/6/429

comprehensive anatomical and functional evaluation of cardiac stenosis and ischemia and pathophysiological understanding of CAD and thus has high clinical relevance.

Acknowledgements The abstract for this paper was submitted to and accepted for the European Congress of Radiology in Vienna 2018. The presentation with the title *Motion elimination in low-dose 4D myocardial computed tomography perfusion (CTP) using the automated smooth temporal registration for analysis of 4D image data (ASTRA) algorithm* (B-0762) was held in the session *New CT protocols to assess coronary artery and myocardium* (SS 703) on the 1st of March 2018.

Funding Prof. Dewey has received grant support for this study from the Heisenberg Program of the DFG (DE 1361/14-1).

Compliance with ethical standards

Guarantor The scientific guarantor of this publication is Prof. Dr. Marc Dewey.

Conflict of interest The authors of this manuscript declare relationships with the following companies:

Prof. Dewey has received grant support from the Heisenberg Program of the DFG for a professorship (DE 1361/14-1) and the FP7 Program of the European Commission for the randomized multicenter DISCHARGE trial (603266-2, HEALTH-2012.2.4.-2).

Prof. Dewey has received lecture fees from Toshiba Medical Systems, Guerbet, Cardiac MR Academy Berlin, and Bayer (Schering-Berlex).

Prof. Dewey is the editor of the Cardiac Section of European Radiology.

Institutional master research agreements exist with Siemens Medical Solutions, Philips Medical Systems, and Toshiba Medical Systems. The terms of these arrangements are managed by the legal department of Charité – Universitätsmedizin Berlin.

Other authors declared no conflicts of interest.

Statistics and biometry No complex statistical methods were necessary for this paper.

Informed consent Written informed consent was obtained from all patients included in this study.

Ethical approval Institutional Review Board approval was obtained.

Study subjects or cohorts overlap Study subjects have been previously reported in Feger et al [12].

Methodology
• Retrospective

References

1. Napp AE, Haase R, Laule M et al (2017) Computed tomography versus invasive coronary angiography: design and methods of the pragmatic randomised multicentre DISCHARGE trial. Eur Radiol 27:2957–2968
2. Bamberg F, Becker A, Schwarz F et al (2011) Detection of hemodynamically significant coronary artery stenosis: incremental diagnostic value of dynamic CT-based myocardial perfusion imaging. Radiology 260:689–698
3. George RT, Jerosch-Herold M, Silva C et al (2007) Quantification of myocardial perfusion using dynamic 64-detector computed tomography. Invest Radiol 42:815–822
4. So A, Wisenberg G, Islam A et al (2012) Non-invasive assessment of functionally relevant coronary artery stenoses with quantitative CT perfusion: preliminary clinical experiences. Eur Radiol 22:39–50
5. Varga-Szemes A, Meinel FG, De Cecco CN, Fuller SR, Bayer RR 2nd, Schoepf UJ (2015) CT myocardial perfusion imaging. AJR Am J Roentgenol 204:487–497
6. de Jong MC, Genders TS, van Geuns RJ, Moelker A, Hunink MG (2012) Diagnostic performance of stress myocardial perfusion imaging for coronary artery disease: a systematic review and meta-analysis. Eur Radiol 22:1881–1895
7. Rief M, Chen MY, Vavere AL et al (2018) Coronary artery disease: analysis of diagnostic performance of CT perfusion and MR perfusion imaging in comparison with quantitative coronary angiography and SPECT-multicenter prospective trial. Radiology 286:461–470
8. Takx RA, Blomberg BA, El Aidi H et al (2015) Diagnostic accuracy of stress myocardial perfusion imaging compared to invasive coronary angiography with fractional flow reserve meta-analysis. Circ Cardiovasc Imaging 8(1):e002666
9. Williams MC, Mirsadraee S, Dweck MR et al (2017) Computed tomography myocardial perfusion vs (15)O-water positron emission tomography and fractional flow reserve. Eur Radiol 27:1114–1124
10. Williams MC, Newby DE (2016) CT myocardial perfusion imaging: current status and future directions. Clin Radiol 71:739–749
11. Kikuchi Y, Oyama-Manabe N, Naya M et al (2014) Quantification of myocardial blood flow using dynamic 320-row multi-detector CT as compared with (1)(5)O-H(2) O PET. Eur Radiol 24:1547–1556
12. Feger S, Shaban A, Lukas S et al (2017) Temporal averaging for analysis of four-dimensional whole-heart computed tomography perfusion of the myocardium: proof-of-concept study. Int J Cardiovasc Imaging 33:371–382
13. Li Z, Yu L, Leng S et al (2016) A robust noise reduction technique for time resolved CT. Med Phys 43:347
14. Pisana F, Henzler T, Schönberg S, Klotz E, Schmidt B, Kachelrieß M (2017) Noise reduction and functional maps image quality improvement in dynamic CT perfusion using a new k-means clustering guided bilateral filter (KMGB). Med Phys 44:3464–3482
15. Feng Q, Zhou Y, Li X et al (2016) Liver DCE-MRI registration in manifold space based on robust principal component analysis. Sci Rep 6:34461
16. Hamy V, Dikaios N, Punwani S et al (2014) Respiratory motion correction in dynamic MRI using robust data decomposition registration—application to DCE-MRI. Med Image Anal 18:301–313
17. Huizinga W, Poot DH, Guyader JM et al (2016) PCA-based groupwise image registration for quantitative MRI. Med Image Anal 29:65–78
18. Melbourne A, Atkinson D, White MJ, Collins D, Leach M, Hawkes D (2007) Registration of dynamic contrast-enhanced MRI using a progressive principal component registration (PPCR). Phys Med Biol 52:5147–5156
19. Wollny G, Kellman P, Santos A, Ledesma-Carbayo MJ (2012) Automatic motion compensation of free breathing acquired myocardial perfusion data by using independent component analysis. Med Image Anal 16:1015–1028

20. Mihai G, Ding Y, Xue H et al (2012) Non-rigid registration and KLT filter to improve SNR and CNR in GRE-EPI myocardial perfusion imaging. J Biomed Sci Eng 5:871–877
21. Muenzel D, Kabus S, Gramer B et al (2013) Dynamic CT perfusion imaging of the myocardium: a technical note on improvement of image quality. PLoS One 8(10):e75263
22. Feger S, Rief M, Zimmermann E et al (2015) The impact of different levels of adaptive iterative dose reduction 3D on image quality of 320-row coronary CT angiography: a clinical trial. PLoS One 10: e0125943
23. Techasith T, Cury RC (2011) Stress myocardial CT perfusion: an update and future perspective. JACC Cardiovasc Imaging 4:905–916
24. Cerqueira MD, Weissman NJ, Dilsizian V et al (2002) Standardized myocardial segmentation and nomenclature for tomographic imaging of the heart. A statement for healthcare professionals from the Cardiac Imaging Committee of the Council on Clinical Cardiology of the American Heart Association. Int J Cardiovasc Imaging 18: 539–542
25. Bamberg F, Marcus RP, Becker A et al (2014) Dynamic myocardial CT perfusion imaging for evaluation of myocardial ischemia as determined by MR imaging. JACC Cardiovasc Imaging 7:267–277
26. Bischoff B, Bamberg F, Marcus R et al (2013) Optimal timing for first-pass stress CT myocardial perfusion imaging. Int J Cardiovasc Imaging 29:435–442
27. Yang Z, Silver MD (2015) Denoising method and system for preserving clinically significant structures in reconstructed images using adaptively weighted anisotropic diffusion filter. Google Patents
28. So A, Imai Y, Nett B et al (2016) Technical note: evaluation of a 160-mm/256-row CT scanner for whole-heart quantitative myocardial perfusion imaging. Med Phys 43:4821
29. Modgil D, Bindschadler MD, Alessio AM, La Rivière PJ (2017) Variable temporal sampling and tube current modulation for myocardial blood flow estimation from dose-reduced dynamic computed tomography. J Med Imaging (Bellingham) 4:026002